 CMC, vol.10, no.2, pp.195-216, 2009

Efficient Simulation of Gas Flow in Blast Furnace

P. B. Abhale[1], N. N. Viswanathan[1] and N. B. Ballal[1]

Abstract: Simulation of gas flow in a multilayered non-isothermal packed bed is useful for blast furnace operators in deciding appropriate charging strategy. While using an anisotropic form of Ergun equation to simulate gas flow through such systems, a new solution methodology for non-isothermal gas with varying density flowing through a layered burden has been proposed. This involves handling non-linearity due to gas density variation with pressure and temperature by solving for the square of pressure instead of pressure directly and handling the non-linearity due to $|v|$ term in the Ergun equation by solving linearized form of Ergun equation and updating $|v|$ iteratively. The proposed scheme is capable of predicting the effect of layer structure on gas flow with economy in number of grid points as well as computation time.

Keywords: porous bed, layer structure, Ergun equation, gas flow, blast furnace

Nomenclature

F_1	Viscous resistance term in Ergun equation, (kg/m^{3}s)
F_2	Inertial resistance term in Ergun equation, (kg/m^4)
$F_\perp$	Resistance perpendicular to a layer, (kg/m^4)
$F_\parallel$	Resistance parallel to a layer, (kg/m^4)
$\dot{G}$	Gas mass generation rate per unit volume, (kg/m^{3}s)
L	Length of the bed, (m)
M	Average molecular weight of the gas, (kg/mol)
P	Total pressure of gas, (N/m^2)
P_0	Reference pressure (Eq. 5), (N/m^2)
R	Universal gas constant, (J/mol/K)
T	Temperature of the gas, (K)
a, b, c	Elements in resistance matrix
d_1, d_2	Thickness of layers 1 and 2, (m)

[1] Department of Metallurgical Engineering and Materials Science, IIT Bombay, Powai, India-400076

d_p Average diameter of any solid particle, (m)
n Molar density of gas (mol/m^3)
r Radial coordinate, (m)
v_r, v_z Superficial velocity of gas in r and z direction, (m/s)
v_1, v_2 Superficial velocity of gas in layer 1 and 2, (m/s)
$|v|$ Magnitude of resultant velocity, (m/s)
$\vec{v}$ Superficial velocity vector, (m/s)
z Axial coordinate, (m)

Greek letters

ϕ Normalized square of pressure, (-)
α Relative thickness of two layers, (-)
β Angle made by layer with the horizontal, ($^\circ$)
ε Voidage in a packed bed, (-)
μ_g Viscosity of gas, (Pa.s)
ρ_g Density of gas, (kg/m^3)
φ Sphericity of particle, (-)

1 Introduction

The iron blast furnace is a large counter-current reactor, where iron ore with fluxes and coke are periodically charged from the top to form alternate layers. Hot blast is continuously injected through the tuyeres and liquid products, viz., slag and molten metal, are periodically tapped from the tap hole. There is counter-current heat and mass exchange between the ascending gas and the descending solids and liquids. That makes the furnace very efficient, with around 80-85% heat utilization [Peacey and Davenport (1979)]. The processes taking place inside the furnace were not clear till several furnaces were quenched and dissected in the 1970's [Omori (1987)]. These dissection studies provided several insights into the blast furnace working. The most important discovery made during the dissections was of the fusion zone or the cohesive zone.

The furnace can be classified broadly into five zones, viz., granular zone, cohesive zone, dripping zone, raceway and deadman. All iron ore reduction reactions primarily occur in the granular zone. This zone consists of alternate layers of oxides and coke. Cohesive layers of partially reduced and partially softened oxides form the cohesive zone. Due to the shape of the isotherms, the cohesive zone is often bell-shaped, the top and the bottom surfaces being at the beginning of softening

and the end of melting temperature. These oxide layers get compacted due to softening and become impervious to gas flow. The flow through these impervious ore layers in the cohesive zone is therefore obstructed, forcing the gas to flow radially outwards through the relatively more permeable coke slits. This zone therefore is a gas distributor. The pattern of alternate charging of the ore and coke layers therefore is an important factor in deciding the distribution of gas and hence heat internally. Metal and slag, fully melted in the cohesive zone, trickle down through the slowly descending coke bed in the dripping zone. The permeability in this zone is important for easy flow of the metal and slag. The presence of coke fines and smaller sized coke reduces the permeability which may cause slag hold up and, in extreme cases, flooding. Since coke is primarily consumed by burning in the raceways in front of the tuyeres, the movement of the coke bed is towards this region. The high velocity gas entering through a number of tuyeres distributed uniformly along the circumference pushes the coke particles towards the center, which form the dense region called the deadman.

Gas flow distribution in the blast furnace has a great influence on productivity, fuel consumption and its operational stability [Peacey and Davenport (1979); Omori (1987)]. The distribution of gas is affected by local variation in permeability of the bed. Hence, the most effective way of improving the productivity of the blast furnace is in controlling the radial gas distribution by means of adjusting permeability variation through proper charging sequence.

Understanding fluid flow through packed beds or porous media is very important not only for blast furnace in particular but also in general for many systems such as ground water flow, filtration, heat storage systems, chemical and metallurgical reactors involving granular materials, sintering processes etc. Ergun developed a semi- empirical equation for a unidirectional flow through a packed bed which relates the pressure drop across a packed bed with the average flow rate [Ergun (1952)]. For developing the relation, he used a theoretical frame work wherein the packed bed was considered as a bundle of tubes having equivalent diameter calculated based on the bed voidage and particle size [Bird, Stewart and Lightfoot (1960)]. Subsequently, Ergun equation has remained as the basis for all the models reported in literature to simulate fluid flow through packed bed or porous media.

Broadly, there are three kinds of models presented in the literature to simulate multi-directional gas flow through packed beds, which are based on the vectorized form of the Ergun equation, Navier-Stokes equation and energy minimization principle [Jiang, Khadilkar, Al-Dahhan and Dudukovic (2000)]. In the vectorized form of Ergun equation, only the gradient of pressure and the interphase resistance between the fluid and particles in the packed bed are considered. The terms arising because of viscous as well as inertial forces in the global sense (as contrasted to

the local flow around each particle or inside each pore) are neglected. On the other hand, models based on the Navier-Stokes equations as well as the energy minimization principle, consider all the terms including the Ergun's fluid-particle interphase resistance term.

Many researchers have employed the Ergun equation in vectorial form along with the mass conservation equation (Eq. 1 and 2 respectively) to simulate gas flow through a multidimensional homogeneous packed bed [Radestock and Jeschar (1970, 1971); Stanek and Szekely (1972, 1973, 1974); Poveromo, Szekely and Propster (1975)]:

$$-\nabla P = F_1.\vec{v} + F_2.|\vec{v}|.\vec{v} \tag{1}$$

where,

$$F_1 = \frac{150(1-\varepsilon)^2\mu_g}{(\varphi d_p)^2\varepsilon^3}$$

$$F_2 = \frac{1.75(1-\varepsilon)\rho_g}{(\varphi d_p)\varepsilon^3}$$

$$\nabla.(\rho_g\vec{v}) = \dot{G} \tag{2}$$

Some authors [Vortmeyer and Schuster (1983); Johnson, Kashiwa and Vander-Heyden (1997); Zhu and Cheng (2007)] used models based on the Navier-Stokes equation wherein the fluid-particle inter-phase drag was described as a body force term using the Ergun equation. Others [Ziolkowska and Ziolkowski (1993); Bey and Eigenberger (1997)] used the Navier-Stokes equation by employing an effective viscosity as the adjusting factor instead of using the Ergun equation, so that their measurements can better fit the model.

The models based on the energy minimization principle assume that the flow is governed by the minimum rate of total energy dissipation in the packed bed. Therefore, the cell interface velocity can be calculated by solving the non-linear multivariable minimization problem [Jiang, Khadilkar, Al-Dahhan and Dudukovic (2000)]. However, this kind of models are not applicable to non-linear systems because principle of energy minimization does not hold in some cases and hence detailed verification is needed before considering the 'energy minimization' as the governing principle [Hyre and Glicksman (1997)].

It should be noted that the computational burden involved in employing models based on either the Navier-Stokes equation or the energy minimization principle to systems like blast furnace is significantly higher than those employing the much

simpler vectorized Ergun equation. In this context, a comparative study between results obtained using models based on the vectorized Ergun equation and the Navier-Stokes equation specifically applied to a multilayered packed bed showed that error introduced by neglecting the inertial terms are not significant [Choudhary, Propster and Szekely (1976)]. Hence, in the present study, model based on the vectorized Ergun equation is used.

Various solution schemes have been reported in literature for solving vectorized Ergun equation. Radestock and Jeschar (1970, 1971) predicted flow through a homogeneous packed bed, by solving the above equations directly for the variables P and v, employing the finite difference formulation and iterative solution using successive over relaxation (SOR). Szekely and co-workers [Stanek and Szekely (1972, 1973, 1974); Poveromo, Szekely and Propster (1975)] used the stream function formulation of these equations to predict flow through a cylindrical layered bed. Computation time required while using stream function formulation is much less compared to solving for primitive variables directly. The nonlinear partial differential equation was solved with spatially varying gas density and voidage for each layer of the bed. In such an approach one has to use several grid points in each layer to capture the details of the flow. Number of layers in the blast furnace being large, this necessitates use of very fine grid structure and consequently large computation time. Yagi and co-workers [Yagi and Muchi (1970); Yagi and Szekely (1977); Yagi, Takeda and Omori (1980, 1982); Chen, Akiyama and Yagi (1992); Austin, Nogami and Yagi (1997)] and Sato, Nouchi, and Kiguchi (1998) resolved this problem to an extent by aligning the grids along the layer surfaces. This strategy, however, limits the solution to the case where inclined layers are defined by straight lines in vertical sections. With advances in modern bell-less top technology, ore and coke burden can be layered in various shapes and thicknesses, by adjusting the charging sequence. In a scenario of curved layer profiles, the approach of Yagi and co-workers poses difficulties.

To overcome such problems, Cross and Gibson (1979) proposed a novel methodology wherein flow through layers of isotropic permeabilities is approximated by considering an equivalent anisotropic homogeneous packed bed, in which the resistances in directions parallel and perpendicular to the flow direction are different. In order to take care of the varying slopes of the interface between layers, the modified equations are transformed from the local coordinates aligned with the layers to the global co-ordinate system for each grid point. Subsequently, the velocity term is eliminated to obtain a highly nonlinear equation in terms of pressure. As Cross and Gibson (1979) considered constant density for the gas, the nonlinearity in equation arises primarily due to the $|v|$ term in the Ergun equation (Eq. 1). It should be noted that Cross and Gibson (1979) demonstrated their concept either for highly

viscous flows by neglecting the second term, or for high Reynolds number flows by neglecting the first term in Eq. 1.

In order to consider gas density variation due to pressure and temperature in the layered packed bed one needs to incorporate the equation of state:

$$PM = \rho_g RT \tag{3}$$

In principle, gas density (ρ_g) and velocity (v) can be eliminated from equations 1, 2 and 3, to obtain a single equation in terms of pressure, along the lines of Cross and Gibson (1979). The resulting equation will have two nonlinearities i.e. one due to the $|v|$ term as mentioned earlier and the other due to the equation of state. Discretization of this equation will result in simultaneous non-linear algebraic equations. For efficient simulation, Bennett and Bradley (1991) combined the momentum equation suggested by Cross and Gibson and the equation of state, and solved it simultaneously with the equation of continuity using an iterative scheme. In this paper, an alternative methodology along the lines of Cross and Gibson is being proposed, to capture the effect of gas density variation due to pressure and temperature.

2 Governing equations

The anisotropic packed bed formulation of Cross and Gibson (1979) has been modified in this work to include the viscous term of the Ergun equation. The details are given in Appendix-A. The equivalent resistances in the two directions viz., gas flowing perpendicular ($F_\perp$) and parallel ($F_\parallel$) to layers include both the isotropic resistances of individual layers and their relative thicknesses, 'α'. This anisotropic form of Ergun equation can then be rewritten for inclined layers after coordinate transformation.

$$|v| \begin{Bmatrix} v_r \\ v_z \end{Bmatrix} = \begin{bmatrix} a & b \\ b & c \end{bmatrix} \begin{Bmatrix} -\partial P/\partial r \\ -\partial P/\partial z \end{Bmatrix} \tag{4}$$

where,

$$a = \frac{cos^2\beta}{F_\parallel} + \frac{sin^2\beta}{F_\perp},$$

$$b = \left(\frac{1}{F_\parallel} - \frac{1}{F_\perp}\right) sin\beta.cos\beta,$$

$$c = \frac{sin^2\beta}{F_\parallel} + \frac{cos^2\beta}{F_\perp}$$

and β is the angle between the local normal to the layer and the z direction.

In order to obtain the gas flow profile, one can iteratively solve Eq. 2, 3 and 4 for the primitive variablesρ_g, P and v directly. As the equations are nonlinear, significant under-relaxation is needed for convergence. The $|v|$ term in Eq. 4 poses further difficulty.

Alternatively, one can substitute Eq. 3 and 4 into Eq. 2 to obtain

$$\frac{1}{r}\frac{\partial}{\partial r}\left[r\frac{P_0^2 M}{2RT\,|v|}\left(-a\frac{\partial\phi}{\partial r}-b\frac{\partial\phi}{\partial z}\right)\right]+\frac{\partial}{\partial z}\left[\frac{P_0^2 M}{2RT\,|v|}\left(-b\frac{\partial\phi}{\partial r}-c\frac{\partial\phi}{\partial z}\right)\right]=\dot{G} \qquad (5)$$

where, $\phi = P^2/P_0^2$, 'P_0' being a reference pressure.

3 Boundary conditions

The schematic of all boundary conditions is given in Fig. 1. At the walls and the deadman boundary, the velocity normal to the surfaces is zero. The gas velocity at inlet and the pressure at top boundary are also to be specified. Radial velocity at the axis has to be zero by symmetry. In the case of inclined layers, a condition such as $\partial P/\partial r = 0$ at r = 0, as was done by Cross and Gibson, does not lead to this condition. In fact, this results in the limiting velocity being non-zero at the axis which is non-physical. The proper boundary condition in terms of pressure is obtained by puttingv_r = 0 in Eq. 4:

$$\partial P/\partial r = -(b/a)\partial P/\partial z \qquad (6)$$

4 Solution strategy

It should be noted that the '$|v|$' term in Eq.5 is the source of nonlinearity. In other words, if '$|v|$' is 'known', then it is a linear-elliptic equation in 'ϕ'. Hence, in the present work, an alternative scheme, wherein 'ϕ' and '$|v|$' will be solved iteratively using Eq. 5 and 4 respectively, is proposed. In addition, a sparse matrix solver with the bi-conjugate gradient method [Press, Teukolsky, Vetterling and Flannery (1992)] has been used for solving the linear simultaneous equations, efficiently. The detailed flow chart is given in Fig.2. Under-relaxation needed for convergence while updating the '$|v|$' is about 0.5.

5 Results and discussions

The formulation presented above has been tested for grid sensitivity and has been validated against published results of Yagi, Takeda and Omori (1980). The furnace

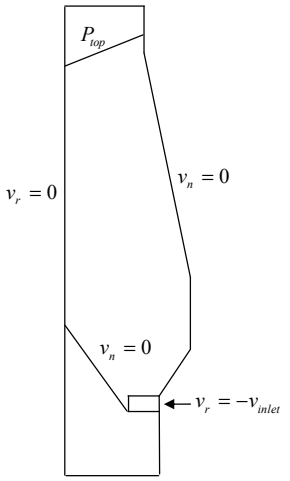

Figure 1: Boundary conditions

dimensions and operating parameters used in these simulations are as shown in Tab.1 and Tab .2.

The blast furnace is divided into five zones namely, lumpy zone, cohesive zone, dripping zone, raceway and deadman. Deadman has been considered as impervious to gas. In lumpy and cohesive zones the bed structure is layered, consisting of alternate oxide and coke layers with the surface angles 28-32° and 33-37°, respectively. The particle diameter, shape factor and voidage used in various zones are given in Tab. 3.

Table 1: Furnace dimensions

Stack diameter	9.5 m	Stack height	18.1 m
Belly diameter	14.6 m	Belly height	3.1 m
Hearth diameter	13.4 m	Bosh height	4.63 m
Throat height	2.0 m	Hearth height	6.07 m

5.1 Grid sensitivity

Sensitivity to grid size has been analyzed by solving the equations for 20x20, 40x40, 80x80 and 160x160 grid points. Selected shapes and positions of different zones of the furnace are shown in Fig.3a. As the grid lengths are halved in both

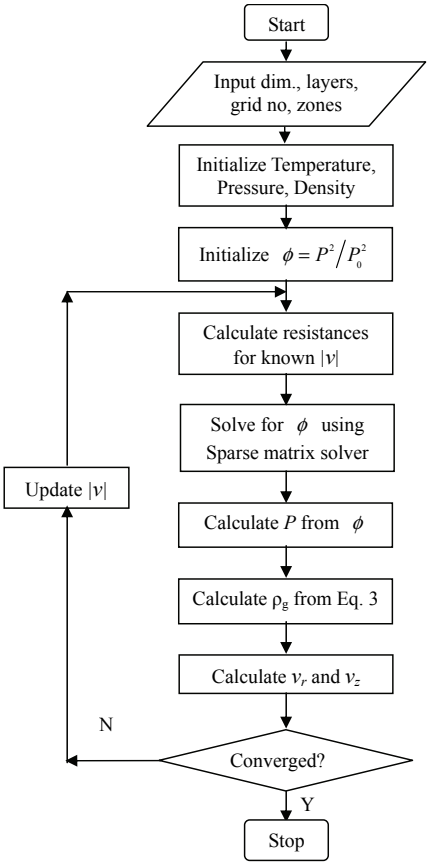

Figure 2: Flow chart of proposed scheme

Table 2: Operating parameters

Top gas pressure	2.75 bar
Blast volume	93.75 Nm^3/s
Top gas temperature	500 K
Blast temperature	1545 K
Production rate	99.97 kg/s
RAFT	2400 K
Surface angle of oxide layer	28-32 °
Surface angle of coke layer	33-37 °

the directions for each succeeding case, one made sure that the boundaries of the

Table 3: Bed properties

Layer/Zone	Particle Dia.(m)	Shape Factor	Voidage
Lumpy zone oxide layer	0.0214	0.84	0.36
Lumpy zone coke layer	0.0477	0.90	0.45
Cohesive zone oxide layer	0.0214	0.84	0.10
Cohesive zone coke layer	0.0477	0.90	0.45
Dripping zone	0.0477	0.90	0.45
Raceway zone	0.0477	0.90	0.80

different zones did not change. Angles and thicknesses of the oxide and the coke layers (Fig.3b) are similar to those employed by Yagi, Takeda and Omori (1980) and show straight lines in vertical sections. The angles and the layer thicknesses are changed from layer to layer, decreasing gradually from the top to the middle of the shaft, and then remained constant below.

Iterations are carried out till the normalized difference between the previous and the current value of '$|v|$' and the mass balance errors for all cells are below 10^{-6}.

The normalized pressure, at some specific locations, obtained for different grid size selections are compared in Fig. 4. Pressures obtained with the finest grids (160x160) have been assumed to have the minimum errors, and therefore have been used to normalize the other pressures in these plots. The errors continuously decrease as the grids are refined, and fall below about 0.3% for the 40x40 grid. Further improvement in the error in the 80x80 grid is marginal.

Predicted wall pressure profiles are plotted as a function of furnace height in Fig. 5. From this it can be observed that in the 20x20 grid the values of wall pressure are under-estimated near the bottom of the furnace and over-estimated above. In the case of the 40x40 grid, the wall pressure values match well with those in the case of the finest grid, except for slight deviation near the root of the cohesive zone. Hence, one can state that about 40 grid points each in the r and the z directions are sufficient to get reasonable accuracy in gas flow predictions.

5.2 Computation time

Computation time required for different selection of grid points while using the proposed scheme is compared with those for the primitive variable approach in Fig. 6. It shows that the computation time required in the latter case is about 1000 times more than that in the scheme proposed, indicating clearly the advantage of the approach taken in the present work.

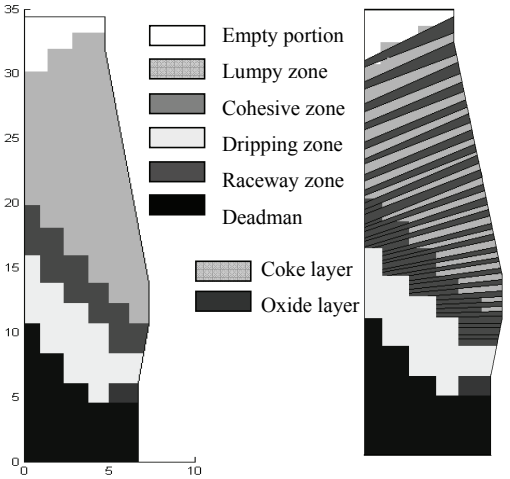

Figure 3: a) Different zones and b) Layer structure used for grid sensitivity

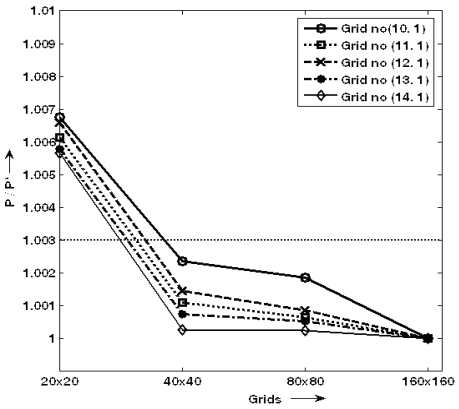

Figure 4: Variation of normalized pressure at specified locations with different grids

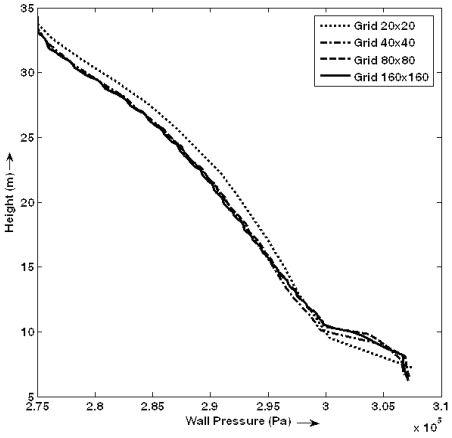

Figure 5: Variation of wall pressure profile with different grids

5.3 Comparison of predictions

As mentioned earlier, Yagi, Takeda and Omori (1980) had simulated flow through inclined layers of ore and coke in a blast furnace using the Ergun equation directly, with the grid structure aligned with the layers. Predictions by the approach taken in the present work are validated by comparison with the results published by them.

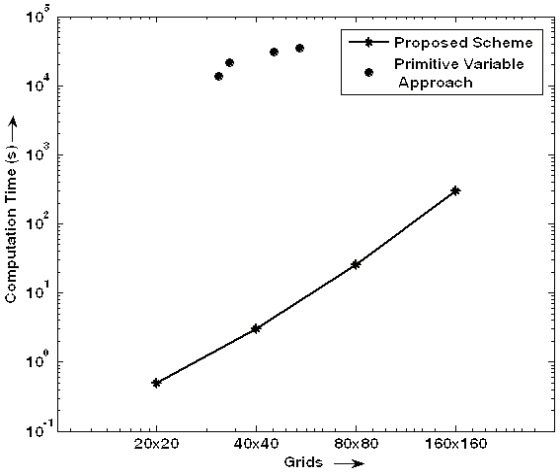

Figure 6: Computation time

The furnace dimensions, operating conditions and bed properties employed for the simulation are same and are given in Tab. 1, 2 and 3. Also, the various zones and the layer structure used are as shown in Fig. 7, which are identical to those used by them. Gas temperatures are varied linearly between 2400K at the raceway level and 300 K at the top. The top gas pressure is 1.67 bar. A 40x40 grid has been employed for the simulation.

In the blast furnace, mass generation in the gas phase occurs primarily in (1) the raceway due to combustion of carbon to carbon monoxide, (2) above the fusion zone by direct reduction of iron oxide leading to generation of carbon monoxide, and (3) in the indirect reduction zone wherein carbon monoxide gets converted to carbon dioxide. In the present study, it is assumed that all the oxygen is converted to carbon monoxide just before it enters the raceway through the tuyeres. About 20% of the total oxide reduction is assumed to take place by direct reduction in a region of about 2 m height above the top of the cohesive zone. Up to this height, the average molecular weight of the gas remains close to 28, as it contains primarily CO and N_2. From here onwards till the top, the indirect reduction zone prevails. In this zone, the number of moles of gas does not change but the average molecular weight changes from 28 to 31 (corresponding to CO_2 of about 19 % at the top). The change in molecular weight with height has been assumed to be linear. Due to this change in molecular weight of the gas, the continuity equation gets modified

as:

$$\dot{G} = \frac{Pv_z}{RT}\frac{dM}{dz} \tag{7}$$

Since, $\nabla \cdot (n\vec{v}) = 0$ i.e. no of moles generated are zero.

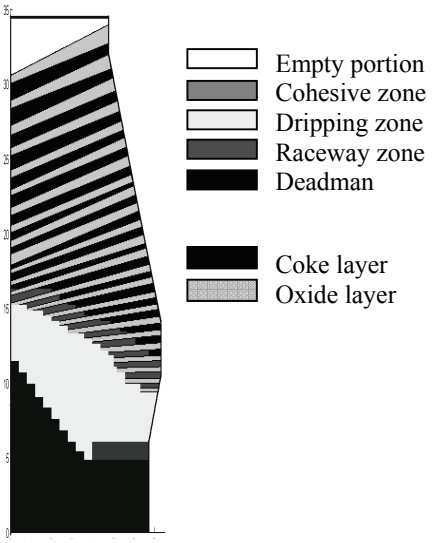

Figure 7: Different zones along with layer structure

Comparison of the predicted wall pressure profile, using all the above conditions, with that reported by Yagi, Takeda and Omori (1980) is as shown in Fig. 8. The wall pressure profiles are in good agreement. Also, one can clearly notice the large change in pressure drop across the fusion zone reflected on the wall pressure profile. As the gas ascends, the axial pressure gradient increases, since the velocity of the gas increases due to decrease in area of cross section for the flow, even as the temperature decreases.

Fig. 9a shows the pathlines followed by the gas starting from the raceway to the top of the furnace, and Fig. 9b shows the vector plot of superficial gas velocity. Gas enters at a velocity of approximately 7 m/s through the slit at the periphery of the furnace. (In a two-dimensional simulation, finite number of tuyeres placed around the circumference need to be replaced by a continuous slit). Since the area available for the gas to flow is increasing in the bosh region the velocity keeps on decreasing. In the cohesive zone, one can clearly see the change in the direction of flow from axial to radial through the coke slits because of the pasty impervious

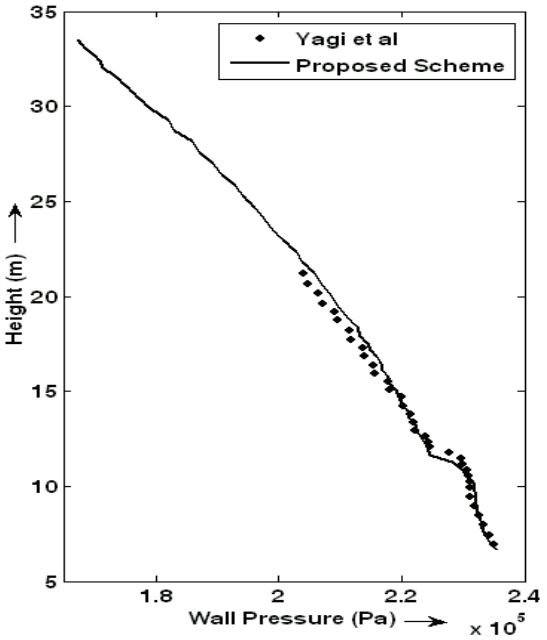

Figure 8: Comparison of wall pressure profile obtained using proposed scheme with that reported by Yagi, Takeda and Omori (1980)

ore layers. In the cohesive zone, adjacent to the wall the gas flow is completely blocked. This forces the gas below the cohesive zone to flow away from the wall, and towards the center. Thereafter, the gas flows through the narrow coke slits with high velocity towards the wall and gets redistributed. In the shaft region, the gas flows in a wavy path due to different voidage in the alternate oxide and coke layers. At the top, the velocity is of the order of 1 m/s. The isobar lines plotted in Fig. 10, show that below the cohesive zone the gas flow is two dimensional, whereas it is mainly axial in the granular zone, and the isobar lines become parallel to layer surfaces. The overall pressure drop is of the order of 1 bar.

5.4 Sensitivity analysis

Simulations have been carried out to explore the effect of ignoring the linear term in the Ergun equation, and the results are shown in Fig.11. It can be seen that about 9% error is introduced in the total pressure drop by ignoring the linear term in the Ergun equation. Considering the fact that gas flow in the blast furnace is in the high velocity (turbulence) regime, the effect of the linear term is noteworthy.

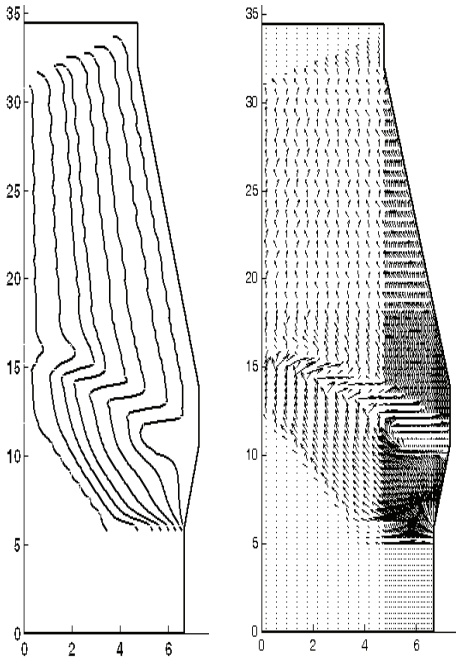

Figure 9: a) Streamlines and b) Velocity vectors obtained using proposed scheme

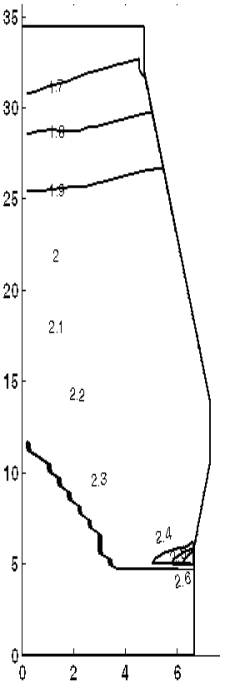

Figure 10: Pressure contours obtained using proposed scheme

This significant contribution may be caused by the accumulation of small errors over almost 25 to 30 m long path traveled by the gas, and the non-linearity of the second term. Assumption made by many researchers in neglecting the viscous term therefore is open to question.

One of the ways of simplifying computation is to ignore local gas generation and instead use an average gas flow rate throughout the furnace. Result of following this approach is compared with that of properly considering the local gas generations is shown in Fig. 12. No significant error in the overall pressure drop is introduced when constant average mass flow is considered. However, the pressure profile is slightly different with larger deviations in the middle part of the furnace.

Similarly, simulations have been carried out (i) with a linear change in temperature from 2400 K at the raceway to 386 K at the top and (ii) a constant temperature of 1200 K throughout, and the results are compared in Fig.13. Evidently, the difference between the two approaches is large, both for the total pressure drop as well as the pressure profile. This may be due to the fact that the quadratic term in Ergun

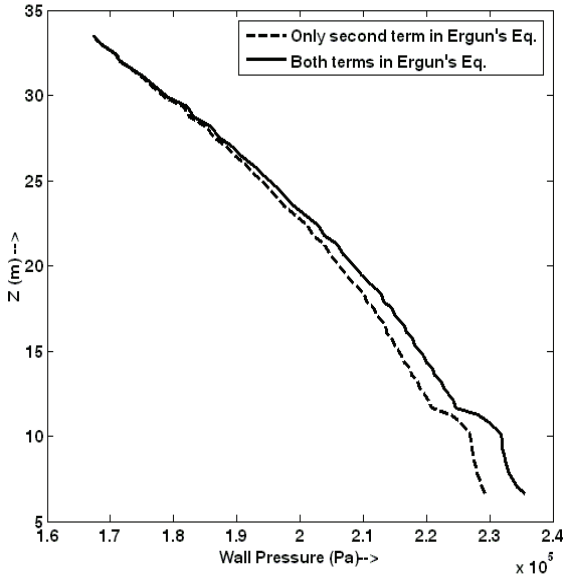

Figure 11: Comparison of wall pressure profiles obtained with and without the linear term in the Ergun equation

equation is dominant in high Reynolds number regime, wherein pressure gradient is directly proportional to '$\rho_g v^2$'. As temperature increases, gas density decreases and to satisfy the continuity ($\rho_g v$=constant) velocity has to increase. In other words, velocity is directly proportional to temperature. Since '$\rho_g v$' is constant, pressure gradient will vary linearly with the velocity and hence with the local temperature.

6 Conclusions

A new approach to obtain non-isothermal compressible gas flow through a layered burden in the blast furnace has been developed. The model using this approach is capable of predicting the effect of alternate layers of ore and coke on gas flow. Simulated results are in good agreement with those reported in the literature. The new approach was able to save considerable amount of computation time due to partial linearization of the equation involved.

It has been shown that the contribution from the viscous term in the Ergun equation is not negligible. Similarly, effect of temperature variation along the height of the bed has been shown to be significant and assuming a constant average temperature for the entire bed may lead to considerable errors.

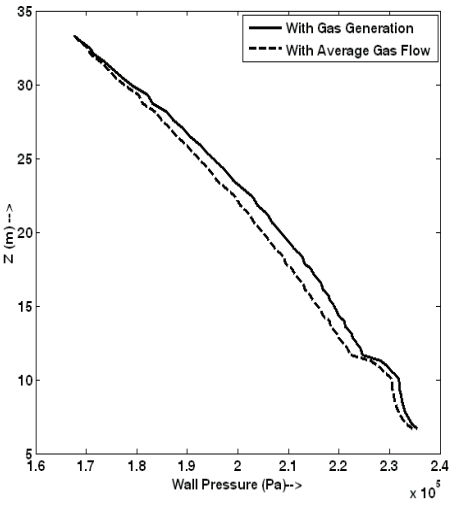

Figure 12: Comparison of wall pressure profiles obtained with local gas generation, and with average mass flow and no gas generation

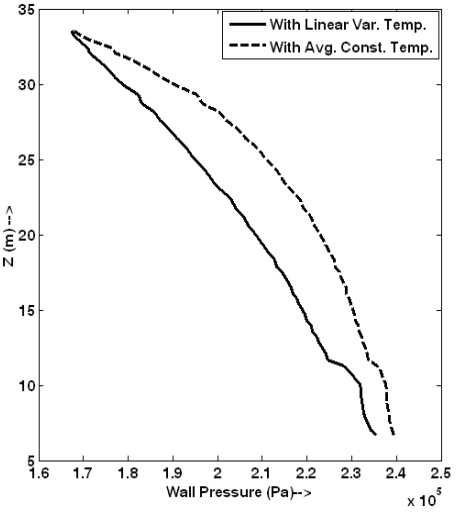

Figure 13: Comparison of wall pressure profiles obtained with linear variation in temperature and with constant temperature

Acknowledgement: Authors would like to thankfully acknowledge the financial support provided by National Metallurgical Laboratory, Jamshedpur, India and Tata Steel Ltd., Jamshedpur, India towards this project.

References

Austin, P. R.; Nogami, H.; Yagi, J. (1997): A mathematical model for four phase motion and heat transfer in the blast furnace, *ISIJ International*, vol. 37, no. 5, pp. 458-467.

Bennett, D. A.; Bradley, R. (1991): Strategy for an efficient simulation of countercurrent flows in the iron blast furnace, *App. Math. Modeling*, vol. 15, October, pp.506-514.

Bey, O.; Eigenberger, G. (1997): Fluid Flow Through Catalyst Filled Tubes, *Chem. Eng. Sci.*, vol. 52, no. 8, pp. 1365-1376.

Bird, R. B.; Stewart, W. E.; Lightfoot, E. N. (1960): *Transport Phenomena*, Wiley, New York, U.S.A.

Chen, J.; Akiyama, T.; Yagi, J. (1992): Effect of burden distribution pattern on gas flow in a packed bed, *ISIJ International*, vol. 32, no. 12, pp. 1259-1267.

Choudhary, M.; Propster, M.; Szekely, J. (1976): On the importance of the inertial terms in the modeling of flow maldistribution in packed beds, *AIChE Journal*, vol. 22, no. 3, pp. 600-603.

Cross, M.; Gibson, R. D. (1979): Gas flow through multilayered regions of porous media, *Powder Technology*, vol. 24, pp. 167-178.

Ergun, S. (1952): Fluid flow through packed columns, *Chem. Eng. Prog.*, vol. 48, no.2, pp. 89-94.

Hyre, M.; Glicksman, L. (1997): Brief communication on the assumption of minimization energy dissipation in circulating fluidized beds, *Chem. Eng. Sci.* vol. 14, pp. 2435–2438.

Jiang, Y.; Khadilkar, M.R.; Al-Dahhan, M.H.; Dudukovic, M.P. (2000): Single phase flow modeling in packed beds: discrete cell approach revisited, *Chem. Eng. Sci.,* vol. 55, pp. 1829-1844.

Johnson, N. L.; Kashiwa, B. A.; Vander Heyden, W. B. (1997): Multi-phase flows and particle Methods (Part-B). *The fifth annual conference of the computational fluid dynamics society of Canada*, May 28–29, British Columbia, Canada.

Omori, Y. (1987): *Blast furnace phenomena and modelling*, Elsevier Applied Science Publishers Ltd., England.

Peacey, J.G.; Davenport, W.G. (1979): *The iron blast furnace*, Pergamon Press Ltd., Oxford, England.

Poveromo, J. J.; Szekely, J.; Propster, M. (1975): Flow maldistribution in the iron blast furnace, *Blast Furnace Aerodynamics Symposium*, *Wollongong*, pp. 1-8.

Press, W. H.; Teukolsky, S. A.; Vetterling, W. T.; Flannery, B. P. (1992): *Numerical Recipes in C-The Art of Scientific Computing*, Cambridge University Press, Second Edition.

Radestock, J.; Jeschar, R. (1970): Ueber die stroemung durch die hochofenshuettung, *Stahl Und Eisen*, vol. 90, no. 22, pp. 1249-1255.

Radestock, J.; Jeschar, R. (1971): Theoretische untersuchung der inkompressiblen und kompressiblen stroemung durch reaktor-schurttungen, *Chem. Ing. Tech.*, vol. 43, no. 6, pp. 355-360.

Sato, T.; Nouchi, T.; Kiguchi, M. (1998): Development of blast furnace operation simulator and its application for reduction of Si content of pig iron, *Kawasaki Steel Technical Report,* no. 38, pp. 24-31.

Stanek, V.; Szekely, J. (1972): The effect of non-uniform porosity in causing flow maldistributions in isothermal packed bed, *Can. J. Chem. Eng.*, vol. 50, no. 1, pp. 9-14.

Stanek, V.; Szekely, J. (1973): Flow maldistributions in two dimensional packed beds- Part II: The behavior of non-isothermal systems, *Can. J. Chem. Eng.*, vol. 51, no. 1, pp. 22-30.

Stanek, V.; Szekely, J. (1974): Three dimensional flow of fluids through non-uniform packed beds, *AIChE Journal*, vol. 20, no. 5, pp. 974-980.

Vortmeyer, D.; Schuster, J. (1983): Evaluation of steady flow profiles in rectangular and circular packed beds by a variational method, *Chem. Eng. Sci.*, vol. 38, no. 10, pp. 1691-1699.

Yagi, J.; Muchi, I. (1970): Theoretical estimation on the longitudinal distributions of process variables in blast furnace and on its productivity, *Trans. ISIJ*, vol. 10, pp. 392-405.

Yagi, J.; Szekely, J. (1977): A mathematical formulation for the reduction of iron oxide pellets in moving beds with non-uniform gas and solids flow, *Trans. ISIJ*, vol. 17, no. 10, pp. 569-575.

Yagi, J.; Szekely, J. (1979): The effect of gas and solids maldistribution on the performance of moving-bed reactors: the reduction of iron oxide pellets with hydrogen, *AIChE Journal*, vol. 25, no. 5, pp. 800-810.

Yagi, J.; Takeda, K.; Omori, Y. (1980): Two-Dimensional Mathematical Analysis of Gas Flow and Heat Transfer in Blast Furnace by the Application of Finite Element Method, *Testu-to-Hagane*, vol. 66, no. 13, pp. 1888-1897.

Yagi, J.; Takeda, K.; Omori, Y. (1982): Two dimensional simulation on the gas flow and heat transfer in the blast furnace, *ISIJ International*, vol. 22, no. 11, pp. 884-892.

Zhu ,Q.; Cheng, S. (2007): 'Redistribution' effect of lumpy zone for gas flow in BF, *J. of Iron and Steel Research, International*, vol. 14, no. 6, pp. 1-7.

Ziolkowska, I.; Ziolkowski, D. (1993): Modeling of gas interstitial velocity radial distribution over a cross-section of a tube packed with a granular catalyst bed, *Chem. Eng. Sci.*, vol. 48, no. 18, pp. 3283-3292.

Appendix-A

Extension of the model proposed by Cross and Gibson (1979) for a layered structure as an anisotropic homogeneous bed considering both linear and non-linear term in the Ergun equation is given below. The resistance for the gas flow parallel to the layer can be modeled as follows:

$$-\left(\frac{\Delta P}{L}\right)_{\parallel} = -\left(\frac{\Delta P}{L}\right)_{L1} = -\left(\frac{\Delta P}{L}\right)_{L2} \tag{A-1}$$

$$-\left(\frac{\Delta P}{L}\right)_{L1} = F_{1,L1}v_1 + F_{2,L1}v_1^2 \tag{A-2a}$$

$$-\left(\frac{\Delta P}{L}\right)_{L2} = F_{1,L2}v_2 + F_{2,L2}v_2^2 \tag{A-2b}$$

Similarly, the overall pressure drop can be written as,

$$-\left(\frac{\Delta P}{L}\right)_{\|} = F_{1,\|}v_{\|} + F_{2,\|}v_{\|}^2 \tag{A-3}$$

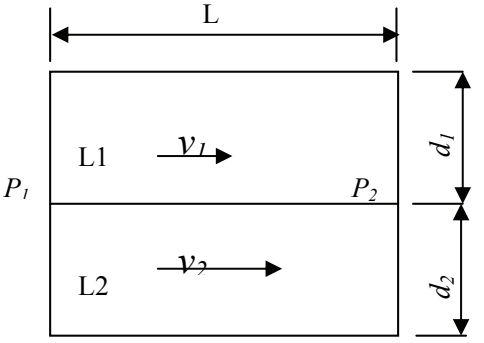

Figure 14: Concept of parallel resistance

As for continuity,

$$d_1v_1 + d_2v_2 = (d_1 + d_2)v_{\|}, \quad \alpha v_1 + (1-\alpha)v_2 = v_{\|} \tag{A-4}$$

Hence, using Eq. A-2, A-3 and A-4, Eq. A-1 becomes,

$$F_{1,\|}\left[\alpha v_1 + (1-\alpha)v_2\right] + F_{2,\|}\left[\alpha v_1 + (1-\alpha)v_2\right]^2 = F_{1,L1}v_1 + F_{2,L1}v_1^2 = F_{1,L2}v_2 + F_{2,L2}v_2^2 \tag{A-5}$$

In the above equation one can separate linear and quadratic terms and eliminate the velocity terms to get,

$$\frac{1}{F_{1,\|}} = \frac{\alpha}{F_{1,L1}} + \frac{1-\alpha}{F_{1,L2}} \tag{A-6a}$$

$$\frac{1}{\sqrt{F_{2,\|}}} = \frac{\alpha}{\sqrt{F_{2,L1}}} + \frac{1-\alpha}{\sqrt{F_{2,L2}}} \tag{A-6b}$$

These two resistances can be combined to get single parallel resistance,

$$-\left.\frac{\Delta P}{L}\right|_{\|} = -\left.\frac{\Delta P}{L}\right|_{1,\|} - \left.\frac{\Delta P}{L}\right|_{2,\|} \tag{A-7a}$$

$$F_{\|} v_{\|}^2 = F_{1,\|} v_{\|} + F_{2,\|} v_{\|}^2 \tag{A-7b}$$

Hence,

$$F_{\|} = \frac{F_{1,\|}}{|v|} + F_{2,\|} \tag{A-7c}$$

Similar analysis for series resistance will give,

$$F_{1,\perp} = F_{1,L1}\alpha + F_{1,L2}(1-\alpha) \tag{A-8a}$$

$$F_{2,\perp} = F_{2,L1}\alpha + F_{2,L2}(1-\alpha) \tag{A-8b}$$

$$F_{\perp} = \frac{F_{1,\perp}}{|v|} + F_{2,\perp} \tag{A-9}$$

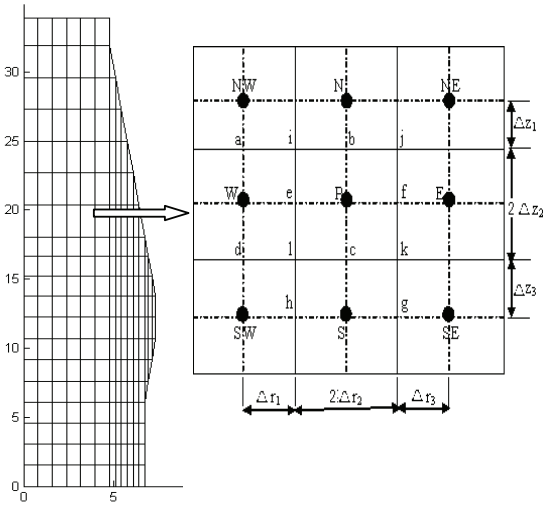

Figure 15: a) Typical grid structure b) Control volume and its neighboring cells

Appendix-B: Discretization

Eq.5 is discretized using the control volume approach. Whole computation domain is divided in to number of orthogonal cells in both r and z direction as shown in Fig. 15a. The staggered control volumes used for discretization are shown in Fig. 15b.

where, 'abcd' forms the control volume for the velocity in r direction, 'efgh' for the velocity in z direction and 'ijkl' for the pressure and the 'ϕ'. The discretized form of Eq. 5 can be written as:

$$a^w A_r^w \left.\frac{\partial \phi}{\partial r}\right|^w + b^w A_r^w \left.\frac{\partial \phi}{\partial z}\right|^w - a^e A_r^e \left.\frac{\partial \phi}{\partial r}\right|^e - b^e A_r^e \left.\frac{\partial \phi}{\partial z}\right|^e$$
$$c^s A_z^s \left.\frac{\partial \phi}{\partial z}\right|^s + b^s A_z^s \left.\frac{\partial \phi}{\partial r}\right|^s - c^n A_z^n \left.\frac{\partial \phi}{\partial z}\right|^n - b^n A_z^n \left.\frac{\partial \phi}{\partial r}\right|^n = \dot{G}.V$$

where, partial derivatives of 'ϕ' which are calculated parallel to the faces i.e. '$\partial\phi/\partial r$'on north and south face, '$\partial\phi/\partial z$' on east and west face, can be obtained by using bi-linear interpolation. Hence, all neighboring cells appear in the final discretized equation.